

# Recent Results from STAR

Markus D. Oldenburg\* for the STAR Collaboration

## 1 The Relativistic Heavy-Ion Collider

The Relativistic Heavy-Ion Collider (RHIC) [1] is situated at Brookhaven National Laboratory (BNL) on Long Island, New York. It has operated since 2000 and delivers protons to Gold (Au) nuclei at a center of mass energy of up to  $\sqrt{s_{pp}} = 500$  GeV for protons and  $\sqrt{s_{NN}} = 200$  GeV for heavy-ions. The two independent accelerator rings have circumferences of 3.8 km.

During the last run period starting in fall 2001 the accelerator was filled with 55–56 bunches of Au ions per ring. Each bunch contained on the average  $7.5 \times 10^8$  Au nuclei at a center of mass energy of 200 GeV per nucleon pair. The peak luminosity was  $5 \times 10^{26} \text{ cm}^{-2} \text{ s}^{-1}$ . In addition we had a very successful polarized proton run at a storage energy of 100 GeV, where RHIC delivered  $0.8 \times 10^{11}$  protons in 55 bunches per ring at a peak luminosity of  $1.5 \times 10^{30} \text{ cm}^{-2} \text{ s}^{-1}$ . The polarization was only around 25%, but we are looking forward to a major improvement in this years run. [2]

At its 6 collision regions RHIC hosts 4 dedicated heavy-ion experiments: Two smaller ones called BRAHMS and PHOBOS, and the two large experiments PHENIX and STAR. In addition the pp2pp experiment will study elastic p-p scattering at high energies.

## 2 The STAR Experiment

STAR focuses on measuring hadronic observables over a wide rapidity range and into a large solid angle. An overall layout of STAR can be seen in Fig. 1. The main detector of STAR is the world's largest time projection chamber (TPC) [3]. A silicon drift detector (SVT) surrounds the interaction vertex. The high (pseudo)rapidity range is covered by two Forward-TPCs (FTPCs). These detectors, which use a radial drift field perpendicular to the applied magnetic field, were developed and built at the Max-Planck-Institut für Physik in Munich [4]. Inside the magnet sits an electromagnetic calorimeter (EMC), which will be fully operational in future runs.

The central trigger barrel (CTB) covers the region around the TPC. It detects particle multiplicity. A pair of calorimeters (ZDCs) at zero degrees

\* Max-Planck-Institut für Physik, Munich, Germany

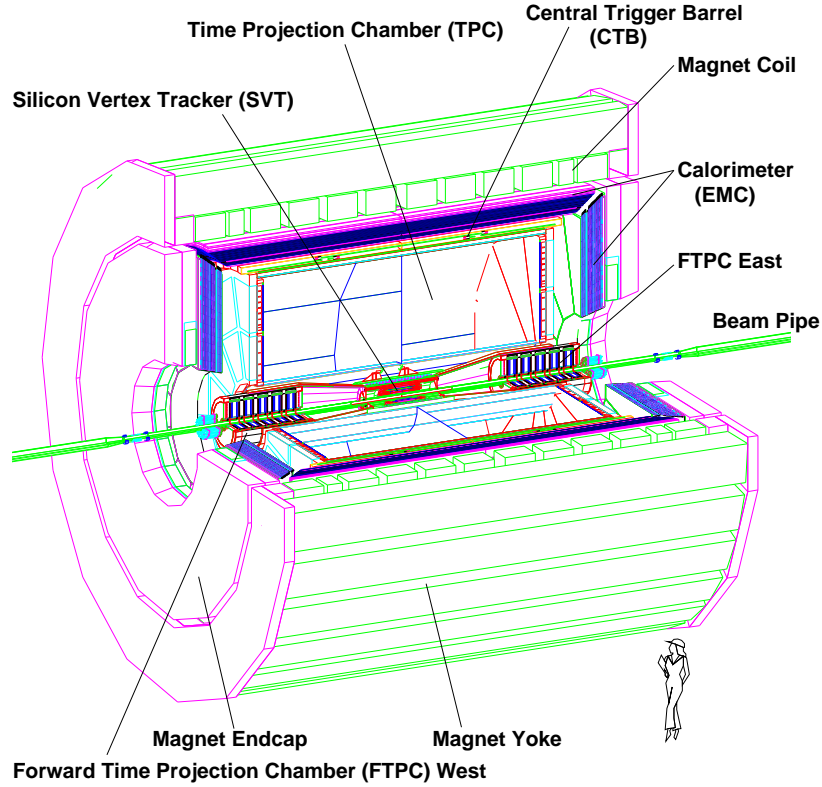


Fig. 1. The STAR detector

with respect to the beam and about 18m away from the nominal collision point measures neutral energy. In combination these two detector types, CTB and ZDC, allow event centrality (or impact parameter) selections.

### 3 Measurements of Anisotropic Flow

Flow produces the anisotropic shape of the transverse momentum distribution in non-central heavy-ion collisions. For its measurement a Fourier decomposition of the momentum distribution with respect to the reaction plane [5] is performed. The reaction plane is given by the beam axis and the closest distance of the centers of the two colliding nuclei. For each event we calculate the Fourier coefficients  $v_n$  for different harmonics  $n$ :

$$v_n = \langle \cos n \cdot (\phi - \Psi_n) \rangle, \quad (1)$$

where  $\phi$  denotes the transverse emission angle of one particle,

$$\phi = \tan^{-1} \frac{p_y}{p_x}, \quad (2)$$

and the reaction plane angle  $\Psi_n$  is estimated on an event-by-event basis by searching for the maxima of the  $\phi$ -distribution.

The 2<sup>nd</sup> Fourier coefficient  $v_2$  is the so called elliptic flow. The ellipticity in spatial coordinates comes about because of the asymmetric overlap of the two colliding nuclei in a non-central collision. However, a finite cross-section for re-interactions is required for this initial state spatial asymmetry to translate itself into a final state momentum space asymmetry; and the cross-sections must be large at early times otherwise the details of the initial collision geometry could not manifest themselves in the final state momentum distributions.

We see elliptic flow in pion, kaon, proton and lambda spectra.  $v_2$  is large and in good agreement with hydrodynamic models for ultra-relativistic heavy-ion collisions [6]. Even the mass dependence is well described by hydrodynamics [7,8]. This is interesting because these models [9] assume local thermal equilibrium and large amounts of elliptic flow can only be generated if equilibrium is established very early in the time history of the collisions.

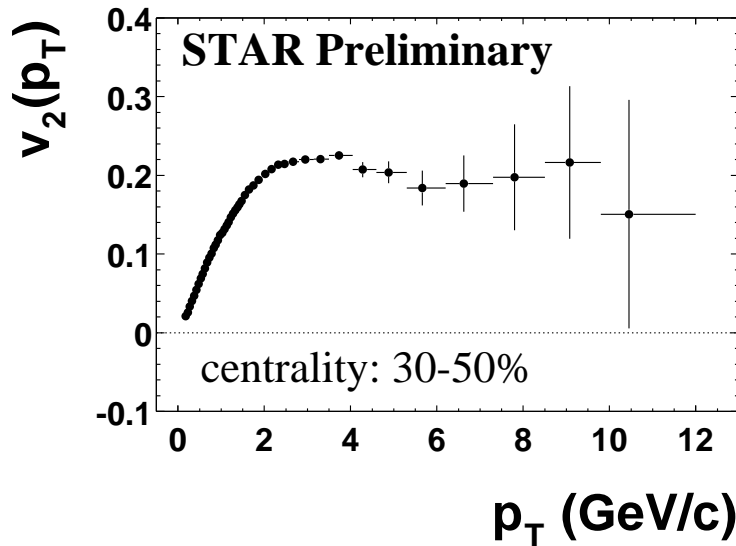


**Fig. 2.** Elliptic flow  $v_2$  as a function of  $p_T$ . At high  $p_T$  the signal saturates which is in qualitative agreement with model calculations [10] assuming partonic energy loss. However, this model implies unnaturally high gluon densities at mid-rapidity

One surprising thing about our data is that elliptic flow persists to high momentum and then it saturates, see Fig. 2. This applies for collision energies of  $\sqrt{s_{\text{NN}}} = 130$  GeV as well as for 200 GeV and for all centralities. The flow pattern follows the prediction of hydrodynamics up to about 2 GeV/c but then hydro predicts that the curve should continue to rise. In contrast we observe that the elliptic flow saturates. Thus, there is some mechanism even at high  $p_{\text{T}}$  which allows the asymmetry in the emission pattern to persist to the highest measured transverse momenta. This mechanism may be partonic energy loss or another exotic process. However, at  $p_{\text{T}} > 6$  GeV/c non-flow effects could have a considerable contribution to the observed  $v_2(p_{\text{T}})$ .

In a model [10] which adds to a perturbative QCD calculation a parameterized hydro component, a similar behavior was observed [11]. There the value of  $v_2(p_{\text{T}})$  at saturation was found to be sensitive to the initial gluon density. This is a hint that the saturation is due to an energy loss of the partons in the dense medium.

## 4 Jets in Nucleus-Nucleus Collisions

Jets are hard to find in heavy-ion collisions because the high multiplicity of particles hides the jets and the calorimeter (EMC) was not completely installed for data taking in 2001. Therefore the question how jets in Au-Au collisions compare to jets in p-p collisions was attacked using a statistical correlation technique. The correlation function is built by identifying a particle with a transverse momentum that exceeds a trigger threshold and then looking for associated high- $p_{\text{T}}$  particles at similar angles and rapidity intervals:

$$C_2(\Delta\phi, \Delta\eta) = \frac{1}{N_{\text{trigger}}} \frac{N(\Delta\phi, \Delta\eta)}{\text{Efficiency}} . \quad (3)$$

The correlation data show that jets exist in central collisions at RHIC and we have previously reported on them at 130 GeV [12]. However, other correlations exist in heavy ion collisions which may not be present in p-p collisions. Elliptic flow is an example. We need a technique to distinguish one correlation from the other.

We have done this by looking in the non-jet region ( $45^\circ < \Delta\phi < 125^\circ$ ) and building up the correlation function in and out of the jet cone. The new correlation function is shown below:

$$C_2(\text{Au} + \text{Au}) = C_2(\text{p} + \text{p}) + A \cdot (1 + 2v_2^2 \cos(2\Delta\phi)) . \quad (4)$$

It includes the p-p correlation and the effects of elliptic flow. The  $v_2$  parameter was determined independently by a reaction plane analysis and the magnitude,  $A$ , of the flow term was fit in the non-jet cone region, see Fig. 3.

The correlation functions for Au-Au and p-p (+ flow) collisions are very similar in the forward jet cone regions ( $|\Delta\phi| < 1$  radian). But the correlation

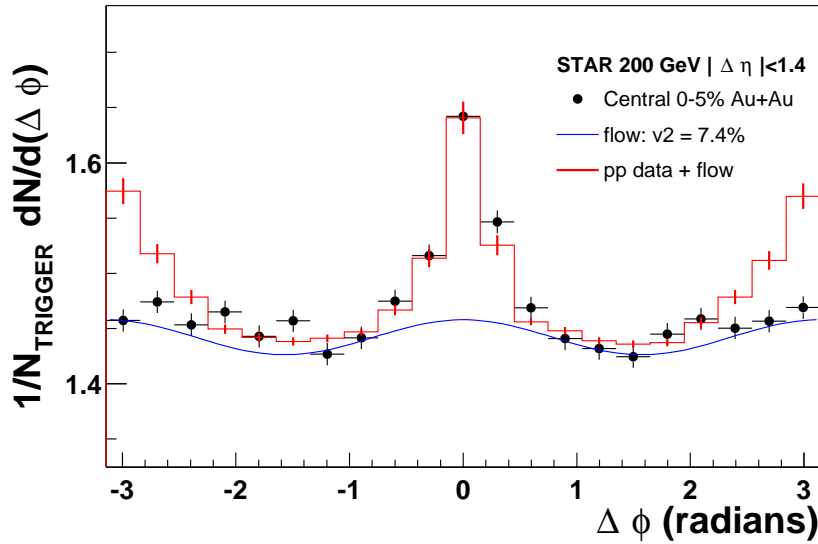


**Fig. 3.** The observed jet like correlation function in heavy-ion collisions is compared to the correlations seen in p-p collisions. The effects of elliptic flow are added to the p-p reference function. Note that the correlation is suppressed at  $180^\circ$  in Au-Au collisions

functions for central collisions are different in the backward cone region and, in particular, the backward going jets in Au-Au are suppressed.

It is possible that a jet can only be seen when it originates near the surface of the collision zone. The backward going jet could be suppressed either because the fireball is opaque to high- $p_T$  particles, or, perhaps, the angular correlation with the away side jets is destroyed by multiple gluon exchange in the gluon saturated core of the fireball.

## 5 Ultra-Peripheral Heavy-Ion Collisions

In ultra-peripheral heavy-ion collisions the two nuclei geometrically ‘miss’ each other and no hadronic nucleon-nucleon collisions occur. At impact parameters  $b$  significantly larger than twice the nuclear radius  $R_A$ , the nuclei interact by photon exchange and photon-photon or photon-Pomeron collisions [13].

We studied exclusive  $\rho^0$  production at  $\sqrt{s_{NN}} = 130$  GeV which, due to the coherent coupling of the exchanged photons to the nuclei, have large cross sections. Furthermore the final states are restricted to low transverse momenta. The Au nuclei are not disrupted, and the final state consists solely of the two nuclei and the vector meson decay products:  $\text{Au} + \text{Au} \rightarrow \text{Au} + \text{Au} +$

$\rho^0 \rightarrow \text{Au} + \text{Au} + \pi^+ + \pi^-$ . In addition to coherent  $\rho^0$  production, the exchange of virtual photons may excite the nuclei:  $\text{Au} + \text{Au} \rightarrow \text{Au}^* + \text{Au}^* + \rho^0 \rightarrow \text{Au}^* + \text{Au}^* + \pi^+ + \pi^-$ .

In general both types of reactions leave you with an ‘empty’ detector, despite of the decay products of the vector meson:  $\rho^0 \rightarrow \pi^+ + \pi^-$ . These two oppositely charged tracks are approximately back-to-back in the transverse plane due to small  $p_T$  of the pair. The Au nuclei remain undetected within the beam (0n, 0n; no up- or downstream neutrons emitted by the nuclei detected). Thus, for  $\text{AuAu} \rightarrow \text{AuAu}\rho^0$  we were triggering on two single hits in opposite side quadrants of the CTB. Because nearly all nuclear decays following photon absorption include neutron emission, for  $\text{AuAu} \rightarrow \text{Au}^*\text{Au}^*\rho^0$  the coincident detection of neutrons in the ZDCs was required (xn, xn).

The spectrum shown in Fig. 4 (a) shows the transverse momentum distribution of pion pairs for the two-track event samples of the minimum bias trigger (xn, xn). It is peaked at  $p_T \sim 50 \text{ MeV}/c$  as is the  $p_T$  spectrum of the (0n, 0n)-triggered events (not shown here). This is the expected behavior from coherent coupling.

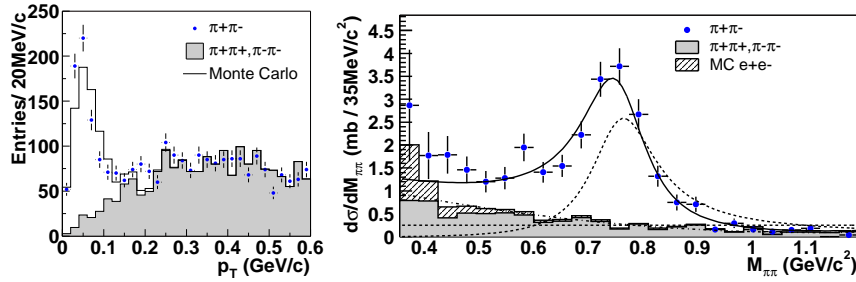


**Fig. 4.** Spectra of coherent  $\rho^0$  production in 2-track events selected by the minimum bias trigger (xn, xn). In both figures points are oppositely charged pion pairs, and the shaded histograms are the normalized like-sign combinatorial background. (a)  $p_T$  spectrum. (b)  $d\sigma/dM_{\pi\pi}$  for events with pair- $p_T < 150 \text{ MeV}/c$ . The hatched histogram contains an additional combinatorial background contribution from coherent  $e^+e^-$  pairs

The  $d\sigma/dM_{\pi\pi}$  invariant mass spectrum for the (xn, xn) events with a pair- $p_T < 150 \text{ MeV}/c$  is shown in Fig. 4 (b); the (0n, 0n) events have a similar  $d\sigma/dM_{\pi\pi}$  spectrum. The spectrum is fitted by the sum of a relativistic Breit–Wigner for  $\rho^0$  production, the contribution of direct  $\pi^+\pi^-$  production and their interference. By extrapolating this fit to full rapidity we measured the cross sections to  $\sigma(\text{AuAu} \rightarrow \text{Au}_{\text{xn,xn}}^* \text{Au}_{\text{xn,xn}}^* \rho^0) = 28.3 \pm 2.0 \pm 6.3 \text{ mb}$ . This value is in agreement with theoretical calculations [14,15]. We estimate  $\sigma(\text{AuAu} \rightarrow \text{AuAu}\rho^0) = 370 \pm 170 \pm 80 \text{ mb}$  (0n, 0n), see [16] for details.

## 6 Conclusions and Outlook

Nuclear matter created by collisions of heavy-ions is not a trivial convolution of nuclear matter created by collisions of protons. Our analyses at 130 and 200 GeV show that the fireball created at RHIC collisions is very dense and possibly opaque. New energy loss mechanisms will be required to explain how high- $p_T$  particles interact with this hot and dense matter.

Our data show that nuclear matter produced at RHIC collisions is accurately described by hydrodynamic models which assume local thermodynamic equilibrium at very early times in the collision sequence. Away side jets appear to be missing in central Au-Au collisions which suggests surface emission of jets or energy loss in the partonic medium. The measurements of coherent  $\rho^0$  production in heavy-nuclei collisions confirm the existence of vector meson production in those reactions and are in agreement with the theoretical expectations.

In summary the properties of nuclear matter at RHIC energies are not inconsistent with local thermal equilibrium. First hints of the predicted jet quenching effect are visible at RHIC. We are looking forward to extend our studies during the upcoming run period which will serve us with up to 29 weeks of d-Au (including cooldown) and 8 weeks of polarized proton collisions.

## References

1. RHIC Conceptual Design Report, BNL Report 52195 (1989)
2. A. Drees, private communication (2002)
3. H. H. Wieman *et al.*, IEEE Trans. Nuc. Sci. **44**, 671 (1997); J. H. Thomas *et al.*, Nucl. Inst. Meth. **A 478**, 166 (2002)
4. K. H. Ackermann, nucl-ex/0211014, to appear in a special volume of Nucl. Inst. Meth. dedicated to the accelerator and detectors at RHIC (2002)
5. A. M. Poskanzer and S. A. Voloshin, Phys. Rev. **C 58**, 1671 (1998)
6. K. H. Ackermann *et al.*, Phys. Rev. Lett. **86**, 402 (2001)
7. C. Adler *et al.*, Phys. Rev. Lett. **87**, 182301 (2001)
8. C. Adler *et al.*, Phys. Rev. Lett. **89**, 132301 (2002)
9. P. Huovinen, P. F. Kolb, U. Heinz, P. V. Ruuskanen, S. A. Voloshin, Phys. Lett. **B 503**, 58 (2001)
10. M. Gyulassy, I. Vitev, and X.-N. Wang, Phys. Rev. Lett. **86**, 2537 (2001)
11. C. Adler *et al.*, nucl-ex/0206006, submitted to Phys. Rev. Lett. (2002)
12. C. Adler *et al.*, nucl-ex/0210033, submitted to Phys. Rev. Lett. (2002)
13. G. Baur, K. Hencken and D. Trautmann, J. Phys. **G 24**, 1657 (1998); C. A. Bertulani and G. Baur, Phys. Rep. **163**, 299 (1988)
14. C. F. v. Weizsäcker, Z. Phys. **88**, 612 (1934); E. J. Williams, Phys. Rev. **45**, 729 (1934)
15. S. Klein and J. Nystrand, Phys. Rev. **C 60**, 014903 (1999); A. Baltz, S. Klein and J. Nystrand, Phys. Rev. Lett. **89**, 012301 (2002)
16. C. Adler *et al.*, nucl-ex/0206004, accepted by Phys. Rev. Lett. (2002)